



Published in final edited form as:

*Spine J.* 2009 September ; 9(9): 744–753. doi:10.1016/j.spinee.2009.04.026.

## Biomechanical Characterization of an Annulus Sparing Spinal Disc Prosthesis

Glenn R. Buttermann, M.D.<sup>1,\*</sup> and Brian P. Beaubien, M.S.<sup>2</sup>

<sup>1</sup> Midwest Spine Institute, 1950 Curve Crest Boulevard, Stillwater, Minnesota 55082

<sup>2</sup> Midwest Orthopaedic Research Foundation, 700 10<sup>th</sup> Ave. South, Minneapolis, MN 55415

### Abstract

**Background Context**—Current spine arthroplasty devices, require disruption of the annulus fibrosus for implantation. Preliminary studies of a unique annulus sparing intervertebral prosthetic disc (IPD), found that preservation of the annulus resulted in load sharing of the annulus with the prosthesis.

**Purpose**—Determine flexibility of the IPD versus fusion constructs in normal and degenerated human spines.

**Study design/Setting**—Biomechanical comparison of motion segments in the intact, fusion and mechanical nucleus replacement states for normal and degenerated states.

**Patient setting**—Thirty lumbar motion segments.

**Outcomes Measures**—Intervertebral height; motion segment range-of-motion (ROM), neutral zone (NZ), stiffness.

**Methods**—Motion segments had multi-directional flexibility testing to 7.5 Nm for intact discs, discs reconstructed using the IPD (n=12), or after anterior/posterior fusions (n=18). Interbody height and axial compression stiffness changes were determined for the reconstructed discs by applying axial compression to 1500 N. Analysis included stratifying results to normal mobile vs. rigid degenerated intact motion segments.

**Results**—The mean interbody height increase was 1.5 mm for IPD reconstructed discs. vs 3.0 mm for fused segments. Axial compression stiffness was  $3.0 \pm 0.9$  kN/mm for intact compared to  $1.2 \pm 0.4$  kN/mm for IPD reconstructed segments. Reconstructed disc ROM was  $9.0^\circ \pm 3.7^\circ$  in flexion-extension,  $10.6^\circ \pm 3.4^\circ$  in lateral bending and  $2.8^\circ \pm 1.4^\circ$  in axial torsion which was similar to intact values and significantly greater than respective fusion values ( $p < 0.001$ ). Mobile intact segments exhibited significantly greater rotation after fusion vs. their more rigid counterparts ( $p < 0.05$ ), however, intact motion was not related to motion after IPD reconstruction. The NZ and rotational stiffness followed similar trends. Differences in NZ between mobile and rigid intact specimens tended to decrease in the IPD reconstructed state.

**Conclusion**—The annulus sparing IPD generally reproduced the intact segment biomechanics in terms of ROM, NZ, and stiffness. Furthermore, the IPD reconstructed discs imparted stability by

\*Corresponding author. Telephone: (651) 430-3800; fax: (651) 430-3827. E-mail address: butte011@umn.edu.

**Publisher's Disclaimer:** This is a PDF file of an unedited manuscript that has been accepted for publication. As a service to our customers we are providing this early version of the manuscript. The manuscript will undergo copyediting, typesetting, and review of the resulting proof before it is published in its final citable form. Please note that during the production process errors may be discovered which could affect the content, and all legal disclaimers that apply to the journal pertain.

maintaining a small neutral zone. The IPD reconstructed discs were significantly less rigid than the fusion constructs and may be an attractive alternative for the treatment of DDD.

## Keywords

Annulus sparing; Axial compression; Artificial spinal disc; Biomechanics; Flexibility; Fusion

---

## Introduction

Spinal fusion is the current treatment for severe lumbar degenerative disc disease (DDD) causing incapacitating low back pain. However, spinal fusion may result in decreased flexibility of the spine and may aggravate degeneration of the adjacent remaining discs which may in turn become painful [1–3]. Spine arthroplasty, which maintains motion segment mobility, may be an alternative treatment option in place of fusion with the goal of avoiding these problems.

Two categories of spine arthroplasty currently exist. One is nucleus replacement, which usually requires an annulotomy for nucleus removal and prosthesis implantation. Most nucleus prosthesis currently in development are manufactured from elastic materials such as a polyvinyl alcohol or polyurethane [4–8]. With these devices, spinal motion occurs either by deformation of the implant (similar to motion through a normal disc) or by rocking of the vertebra over the implant, in which motion is constrained by the remaining annulus, spinal longitudinal ligaments, and facet joints or capsules. Another category of spine arthroplasty is “total” disc replacement in which the anterior and usually the posterior longitudinal ligaments are released, most of the annulus removed and the disc space filled with a device. Most of these devices are mechanical and are positioned into the interbody space. Typically these devices have metallic endplates with porous ingrowth surfaces for fixation to the bony vertebral endplates. Spinal motion occurs by an articulating joint with the motion constrained by the facet joints and remaining lateral annulus [9;10]. Common to both nucleus and total disc prostheses is the need to alter (i.e., excise or transect) the annulus fibrosus. Consequently, the biomechanical function of the annulus, which requires intact circumferential annular fibers, cannot be restored.

Another concept in spinal arthroplasty is the annulus-sparing nucleus replacement, which completely maintains the integrity of the existing annulus. Such a device would have its motion dictated by the normal soft tissue constraints of the intact disc, and would be load-sharing with the surrounding annulus. This theory was supported in one pilot study, which found approximately 40% of the axial load applied to a reconstructed motion segment was borne by an annulus-sparing device [11]. Such load-sharing could result in reduced stresses to the device and its bone interface *in vivo*, which would give it greater longevity and reduced subsidence risk.

To our knowledge, two annulus sparing nucleus replacement devices exist, neither of which is FDA approved: one is an *in situ* curing silicone nucleus device that is implanted via the trans-sacral approach (TranS1 Inc., Wilmington, NC), and the other is a previously described modular intervertebral prosthetic disc (IPD; Dynamic Spine Inc., San Diego, CA); the latter is the focus of this study [12]. The IPD device is implanted via one or two cavities made in the vertebra(e) adjacent to the indicated disc through which the central vertebral endplate and nucleus are excised. The IPD has no articulating parts, instead it comprises an elastic spring component, which is placed in the excised nuclear space, and one or two vertebral body fixation components (Figure 1). The elastic component occupies the nuclear space with the implant area representing approximately 25% of the total disc area. In a prior study using lumbar calf spines comparing a fourfold range of elastic component stiffness; it was found that the implanted device affected the overall biomechanical properties of the reconstructed segment

[12]. In the current study we used the stiffer IPD (160KN/m), which best reproduced bovine intact values to reconstruct human lumbar discs.

One of the first steps in determining the potential clinical applicability of an annulus sparing device was to assess whether the implanted device could approximate the biomechanical properties of intact human lumbar motion segments. Specifically, the purpose of this study was to determine if the elastic component of the implanted IPD in response to applied external loads could reproduce the disc height, axial stiffness and rotational flexibility of the intact human lumbar motion segment. A secondary goal was to stratify the results to normal mobile discs versus the clinically applicable degenerative and more rigid disc cases. An additional objective of was to compare the flexibility of the IPD reconstructed motion segments to fusion constructs which is currently the primary surgical treatment for advanced DDD.

## Methods

Thirty human lumbar motion segments were obtained for from donors with characteristics shown in the Table. All specimens were cleaned of unnecessary soft tissue while retaining the discs, facet capsules, and spinal ligaments; radiographs and bone density measurements were obtained (DEXA). Motion segment degeneration was classified radiographically [13–16]. The spines were dissected to obtain L23 and L45 motion segments (IPD group n=6 L23 and 6 L45; fusion group: n=9 L23 and 9 L45). A larger number of specimens were assigned to the fusion group as this was required for a subsequent study of supplemental anterior lumbar plates. The outer endplates were fixed with supplemental screws, potted in urethane epoxy and stored at  $-20^{\circ}\text{C}$  until testing. Once thawed, specimens were kept moist between tests with 0.09% saline spray and a plastic film wrap.

Axial compression testing was performed on the IPD group using a sinusoidal waveform to 1,500 Newtons (N) at mean rates of 8, 80, and 800 N/sec over three cycles and with a 10-sec dwell time between cycles. The segments were constrained in all other translations and rotations during compressive loading so that height changes could be accurately measured.

Flexibility testing was performed with unconstrained moments in all anatomic planes as previously described [17]. Sagittal bending (flexion/extension), lateral bending and axial torsion were applied sinusoidally to  $\pm 7.5$  Newton-meters (Nm) at 0.04 Hz, with an additional 100-N axial compressive load coincident with the long axis of the distal vertebrae. This compressive load level was chosen to ensure the device was always under some compression, but was small relative to body weight in order to minimize the artifact that occurs with preload application [18].

Reflective spheres mounted on the proximal and distal vertebral bodies were tracked with an infrared video motion measurement system (Vicon, Oxford Metrics, Oxford, UK) and their motions were reduced to rigid body rotations using Euler angle formulations. All tests were repeated three times with a 10-sec dwell time between loading cycles; only the third cycle was used for data analysis. The sequence of load state testing (flexion/extension, lateral bending, and axial rotation) was varied among the specimens.

All load-testing states were repeated with the IPD reconstructed disc both with and without simulated fibrous tissue, which has been shown to grow between the spring coils of the IPD in a pilot *in vivo* animal study [19]. In the current study, fibrous tissue was simulated with a household silicone with an elastic modulus of approximately 0.9 MPa (Silicone II, General Electric, Waterford, NY), which is greater than but within an order of magnitude of that reported for other predominantly Type I collagen fibrous soft tissues [20]. Ingrowth was simulated by applying the silicone between the spring coils of the elastic component, which is made of four springs. Implantation of the IPD first required making a cavity in the vertebral

body adjacent to the disc to be reconstructed. Clinically, the approach may be made directly anteriorly, anterolaterally, or direct laterally (as recently demonstrated in large animal studies [19]). For the present study an anterolateral approach was used as this most familiar to surgeons for performing anterior interbody fusion. A cutting guide was temporarily attached to the anterolateral vertebral body adjacent to the disc to be reconstructed, a cortical window was cut after which a depth-controlled reamer removes cancellous bone to make a cavity. The width of the window was 25 mm corresponding to the diameter of the IPDs, which were sized for the motion segments tested (mean coronal endplate diameter of 57 mm, mean sagittal endplate diameter of 40 mm). Specialized instruments, which included a right angle hole-saw, were used under fluoroscopic guidance to make reproducible and accurate bony endplate cuts and core out and remove the central endplate and nucleus, thereby leaving the annulus intact. The degree of degeneration of the excised nucleus was qualitatively graded (grades 1 = normal to 5 = advanced degeneration) [21]. The IPD was implanted by first placing the elastic component through the cavity in either vertebral body into the excised nucleus space, and then securing the fixation components to the elastic component. The expandable fixation components were elongated using a calibrated, load-indicating tensioner until a 100- to 125-N preload was applied. The preload force on the elastic component results in distraction between the two vertebral bodies and restoration of the disc height, and gives immediate stability to the fixation components within the vertebral body cavities. The elongated fixation components were then secured in the elongated position; a lateral flange on the fixation component gives the device cortical support. Clinically, and as shown by an animal study, the bone removed during creation of the vertebral cavities is replaced, and this bone is expected to heal rigidly back to the vertebral body bone and to the porous ingrowth surface of the fixation components thereby providing long-term stability [19].

The fusion group also had flexibility testing repeated after a combined anterior/posterior instrumented fusion construct. These specimens had a subtotal anterior discectomy and cartilaginous endplate removal performed, and a prosthetic interbody cage (spacer) placed that was a minimum of 2 mm oversized in height to distract the disc space for a tight fit. Posterior instrumentation was with 6.5 mm diameter pedicle screws and 5.5mm diameter titanium rods (Abbott Spine, Austin, TX, USA).

Range of motion, neutral zone, initial stiffness and elastic zone stiffness were calculated from the moment-rotation data. From the moment-rotation curves, the range of motion was defined as the total amount of motion, and neutral zone was defined as the difference in rotation after unloading in the positive vs. negative rotation directions. Stiffness was defined as the slope of the tangent of the load-displacement curve, and was calculated in the initial (i.e., in the low-moment semi-linear region) and the elastic zone (i.e., in the high-moment semi-linear region) regions. The stiffness in axial compression was determined at the 0- to 400 N level to represent the initial stiffness, and at the greater than 400 N level to reflect the loads experienced in many activities of daily living [22;23].

Statistical analysis was performed for all load states to compare intact discs and IPD reconstructed discs with and without silicone and fusion constructs. Differences in disc height, range of motion, neutral zone and stiffness were analyzed. Statistical comparisons were made using a repeated measures analysis of variance with the Tukey adjustment for multiple comparisons. Probability values of less than 0.05 were considered statistically significant. Error bars on the graphs represent plus or minus one standard deviation.

Analysis was also performed to evaluate the effect of the intact segment mobility on postoperative mobility. Two subgroups were analyzed based on the intact flexion-extension range of motion. One group consisted of the upper 50<sup>th</sup> percentile and the other of the lower 50<sup>th</sup> percentile of the flexion-extension range of motion of the combined IPD and fusion groups.

The median value of 9 degrees ROM represented the division point, which also has clinical relevance when considered in the context of clinical vertebral mobility, and when compared to a prior study which evaluated the relationship of ROM vs. degeneration [24]. Differences in range of motion, neutral zone and demographic data were compared between reconstructed disc values (fusion or IPD) and the respective intact values were calculated. These differences were compared using a two-way ANOVA with mobility (rigid or mobile) and treatment (IPD or fusion) as factors. Pairwise comparisons were made using the Tukey method.

## Results

In the fusion group mobile segments tended to come from donors that were younger and heavier with greater disc heights and greater disc height/sagittal diameter ratios. The intact segments from the IPD group exhibited similar trends (see Table). The motion segments were from larger donors for the IPD group but when normalized by the disc height/sagittal diameter ratio, they were similar to the fusion group. There were no clear trends in terms of DEXA score or radiographic degeneration levels. Statistical comparisons on the combined fusion/IPD intact segment data revealed statistical differences only for the visual disc degeneration grade ( $p=0.046$ ), which was lower (less degenerated) for the mobile segments, and disc height/diameter ratio ( $p=0.003$ ), which was greater for the mobile segments. Non-significant comparisons had a low power ( $<0.3$ ) for this sample size.

For the IPD group, device implantation increased unloaded disc height by  $1.5 \pm 1.1$  mm (mean  $\pm$  standard deviation) compared to the respective intact state. The disc height increase for the circumferential fusion group was  $3.0 \pm 1.8$ .

For all states the axial compression load-displacement curves at testing rates of 8, 80, and 800 N/sec revealed a nonlinear response that was similar at 80 vs. 800 N/sec loading rates, but greater in displacement at 8 N/s (Figure 2). A load rate of 80 N/s was used in the following comparisons. Axial compressive stiffness of intact motion segments was  $1.46 \pm 1.07$  kN/mm and  $3.01 \pm 0.86$  kN/mm at applied loads less than and greater than 400 N, respectively. Axial compressive stiffness of the IPD reconstructed discs was  $0.38 \pm 0.22$  kN/mm and  $1.02 \pm 0.32$  kN/mm at low and high loads, respectively. IPD reconstructed discs with simulated fibrous tissue axial stiffness was  $0.56 \pm 0.27$  kN/mm and  $1.15 \pm 0.38$  kN/mm respectively. The difference in stiffness between the intact and reconstructed discs was statistically significant in both the high and low load regions ( $p<0.001$ ). The fusion constructs, with the connecting rods removed so as to compare the interbody device alone (with deficient annulus due to the annulotomy) to the IPD with intact annulus, had an axial compressive stiffness of  $0.81 \pm 0.28$  kN/mm which was linear ( $r^2 = 0.994$  to  $0.999$ ) at  $<400$  N. Axial compression stiffness determination for the fusion constructs in the 400N to 1500N range was not valid since a number of the fusion cages subsided.

Intact and IPD reconstructed motion segments produced flexibility (i.e., moment-rotation) curves with the characteristic sigmoidal shape as illustrated in Figures 3–5. The IPD group range of motion (ROM) in combined flexion-extension was  $8.7^\circ \pm 4.5^\circ$  for intact segments and  $9.0^\circ \pm 3.7^\circ$  for IPD with simulated fibrous tissue range-of-motion; neither IPD with or without silicone differed significantly from intact ( $p>0.05$ ). In bilateral lateral bending the ROM was  $8.9^\circ \pm 2.5^\circ$  for intact segments and  $10.6^\circ \pm 3.4^\circ$  for the IPD with simulated fibrous tissue; both IPD and IPD with simulated fibrous tissue had significantly increased values relative to intact ( $p = 0.003$  and  $0.009$ , respectively). In axial torsion, the ROM was  $1.8^\circ \pm 1.1^\circ$  for intact segments and  $2.8^\circ \pm 1.4^\circ$  for IPD with simulated fibrous tissue; in rotation the ROM was greater for the IPD vs. intact segments ( $p=0.03$ ). The NZ followed similar trends, but did not differ for intact vs. reconstructed segments ( $p>0.2$ ). Within the IPD group, rigid intact segments did



not result in reconstructed motion segments having decreased range of motion or neutral zone vs. those reconstructed from more mobile intact segments ( $p>0.2$ , Figures 6–8).

No intact vs. IPD differences in initial stiffness were statistically significant. For the elastic zone stiffness, global differences were marginally significant in lateral bending ( $p=0.054$ ), but differences in axial torsion were statistically significant for intact vs. the IPD ( $p = 0.008$ ) and IPD vs. IPD with simulated fibrous tissue ( $p=0.028$ ), but not for intact vs. IPD with simulated fibrous tissue (Figure 9).

The reference, fusion group was more rigid vs. the intact disc in terms of ROM, and stiffness in all directions ( $p<0.001$ ), except in torsion neutral zone. Fusion constructs provided a greater reduction in ROM and neutral zone vs. the intact segment than did the IPD in all directions ( $p<0.001$ ) except torsion neutral zone, where global significance was not achieved. Segments with the fusion constructs revealed that segments that were more rigid in the intact state resulted in a lower ROM in all directions ( $p 0.043$ ), and in terms of flexion-extension neutral zone ( $p=0.002$ , Figures 6–8).

## Discussion

This study is the first to evaluate a mechanical annulus-sparing nucleus prosthesis (IPD) in a human lumbar spine model. Anterior disc height of intact lumbar discs were similar to that previously reported [25–27]. The fusion constructs all had oversized interbody cages to “overstuff” the disc space to maximize rigidity and thus routinely had an increase in disc height. To varying degrees, all discs had an increase in disc height vs. the intact disc after implantation with the IPD. Increased disc height and nuclear space volume would likely produce an outward bulge of the ingrown fibrous tissue under axial loading of the IPD. Radially bulging fibrous tissue will likely apply a radial force on the inner surface of the spared annulus, which in turn will place the intact annulus under circumferential stresses (in the general direction of its collagen fiber bundles), as does the normal annulus. This may contribute to additional load sharing and enhance the health of the annulus [28–31].

Axial compression testing of the intact human lumbar motion segments tested in this study found axial deformation (i.e., a decrease in disc height) to be in the range previously reported for human lumbar discs, which is approximately 0.2 to 1.8 mm at 500N to 1200N applied load [32–36]. IPD reconstruction of the discs maintained original disc height and often slightly increased it in the unloaded state. Axial compressive stiffness of the human IPD reconstructed segments was less than that of the intact segments of this study, but within the range of prior reports, which range from 0.3 to 4.0 kN/mm [33;36–41]. Testing at low vs. high applied loads in prior studies has also found stiffness to be nonlinear, and it should also be noted that the upper range reported for human data often reflects testing of some older specimens, which are characterized by disc height collapse and osteophytes. In the present study, none of the discs had advanced disc degeneration.

One reason that the low load axial stiffness was less in the reconstructed discs of the present study may be that the device is inserted in the absence of applied loading. As the device is implanted and expanded the disc height increases and the annulus is tensioned vertically. Loading applied to the reconstructed segment may have then resulted in an initial compression of the device and height loss of the disc, which would allow the annulus to be first relaxed and then engaged as it is compressed and stiffened. With the annulus engaged in the high load region (i.e., above 400N, or approximately body weight) the stiffness was within the range previously reported (above) for intact human motion segments. Published axial compression data for disc replacements are few. One previous report of a hydrogel type nucleus prosthesis tested in human cadavers and implanted via an experimental annulus sparing technique had

similar axial stiffness to that in the present study [42]. Another prosthetic (total) disc which is non-articulating and made of fiber reinforced polymers also had an axial compressive stiffness that was similar to the device described in the current study [39].

The range of motion of the intact human lumbar motion segment has also been studied, and approximate values are reported to be 5–13° in flexion, 2–5° in extension, 3–6° in right or left lateral bending, and 1.3–2.2° in clockwise or counterclockwise axial torsion [40;43–51]. Decreased range of motion of our intact specimens correlated with gross morphologic disc degeneration but not with plain radiographic disc degeneration which has been previously noted [52,53]. For the IPD reconstructed specimens tested in the present study, statistically significant differences existed in terms of lateral bending ROM and axial torsion elastic zone stiffness relative to the intact state. However, the ROM values (total arc of motion) for all states were within the above ranges found in intact motion segments of the above prior studies. Neutral zones of intact and reconstructed discs were similar and were within ranges given in the above previous reports. Stratification between mobile (representing normal) and rigid (representing degenerated) intact motion segments found that after IPD reconstruction that the more mobile segments maintained the intact neutral zone. This suggests that the IPD imparts a degree of stabilization [54]. Reproducing a near normal neutral zone is important as it reflects motion segment stability and may be clinically relevant [55,56]. Conversely the more rigid intact specimens tended to have a small increase in neutral zone and flexion-extension ROM which tended to bring all segments to a similar degree of flexibility. As expected, the fusion specimens were significantly more rigid than the intact and IPD reconstructed specimens.

Rotational stiffness for human lumbar motion segments ranges from less than 0.5 to over 8 Nm/degree in bending and, owing to the facet joints, axial torsion stiffness has been reported to be as high as 18.8 Nm/degree [40,45,46,48]. Interpreting stiffness of a spinal unit depends on the load-displacement region that is being studied, because stiffness for both axial and rotational loading typically increases at greater applied loads. In this study we reported the initial (low-load region) stiffness and the elastic zone stiffness (high-load region). The IPD reconstructed discs were similar to intact discs in this study, as well as that previously reported for intact discs, in both initial and elastic zone stiffness except for axial torsion which was slightly less in this study. Some of the variability in stiffness of the IPD reconstructed disc motion segments may reflect a loss of preload of the implant during the duration of the testing. This has been noted previously using interbody fusion devices [57].

Limitations of this study include those inherent to *in vitro* testing and others specific to our methodology. The *in vitro* tests were performed to simulate the immediate post-operative state and thus did not represent bone ingrowth at the device-endplate junction; such *in vivo* ingrowth would likely enhance stability of the IPD and possibly reduce flexibility of the reconstructed segment. Another limitation is that the silicone used to simulate fibrous tissue was fully enclosed within the diameter of the device, and did not imbibe water. Fibrous tissue formed *in vivo* would likely grow within the implant but may also extend to and exert outward pressure upon the inner annulus, thereby stiffening the segment, and a high water content would likely make the motion segment response more rate-dependent. The compressive testing was performed in this study in an otherwise fully-constrained fashion. Less constrained conditions would likely have followed similar trends, but may have allowed re-alignment under loading and may have produced somewhat different segmental stiffness values. Few inter-group differences were found due to the similarity of the average specimen response, but also due to the varying response of the specimens to treatment and the resulting low statistical power. The response to IPD reconstruction may have differed due to surgical or implantation variables or the varying specimen stiffness with respect to the IPD device stiffness. Finally, with regard to the present study, the fact that the intact specimen was always tested first may have introduced time or order-related effects [58] There are potential clinical concerns, one is the potential

anatomical mismatch of the device to the high lordotic angulation of some L5S1 discs and the location of vascular structures such as when the iliac bifurcation is low. Another clinical concern is the size of the bone window required to implant the device and the size of the fixation components which may weaken the vertebral body or make revision difficult. The present study investigated primarily the implanted elastic component. The concern regarding the fixation component apparently is being addressed by the manufacturer by using only a single fixation element and alternative materials. Pilot large animal studies focusing on the fixation component have found reliable bone healing of the bone window and implant stability despite *in vivo* loads of over 2.5 MPa [19]. This *in vivo* pilot data suggests that the fixation component acts as a vertebral body replacement to reinforce the instrumented vertebra and that the axial compressibility of the flexible component load shares with the annulus and facet joints as suggested in prior *in vitro* testing [11]. Pilot destructive axial compression testing results suggest the IPD has greater construct stability than stand-alone fusion devices of which many were found to subside at loads between 400 N to 1500 N. Aside from the fixation component concerns, the testing results of the device used in this study should still be relevant since the elastic component is what allows motion and compressibility.

A comparison may be made with the *in vitro* flexibility results of the IPD reconstructed discs in this study to other devices currently under investigation. Prior *in vitro* studies have found variation in total disc kinematics. One total articulating type of disc replacement tested at the L5-S1 level to 10 Nm found flexion/extension, lateral bending, axial torsion range of motion of 2.5°, 6.8°, and 1.8° respectively [59]. This is less than the values of the current study, as well as that reported by others which found 10° to 13° flexion/extension at 6 to 8 Nm applied moments for total disc prostheses [60–62]. The variable results of these other studies may be due to the condition of the human tissue that was used, the amount of distraction to fit oversized implants into narrow disc spaces, and the amount of annulus and longitudinal ligament resection [63]. The device evaluated in this study represented an annulus- and ligament-sparing design. Preservation of these soft tissues may be important for motion segment stability, particularly when used in multi-level disc arthroplasty [64].

This paper focused on the basic biomechanical properties of IPD reconstructed compared to intact and fused motion segments. The mechanical IPD tested in the present study spares the annulus, is elastic but was also designed for rigid fixation to the adjacent vertebrae in contrast to other devices which are enclosed in the nuclear space. The rotational load-displacement relationship of human lumbar motion segments with discs reconstructed with an IPD was generally similar to that of the intact state in terms of flexibility parameters and overall stiffness. Additionally, discs reconstructed with an IPD seemed to find a middle ground for ROM and neutral zone for motion segments that were originally mobile vs rigid. This justifies further investigation, including additional comparative studies that quantify the helical axis of rotation (quality of motion), load sharing of the IPD with the annulus and facet joints, and destructive failure testing in compression, rotation and shear modes which would be relevant to whole-disc mechanics, subsidence risk and device longevity.

## Acknowledgments

Funded by NIH (grant no. 1 R43 AR048732-01A1).

## Reference List

1. Gillet P. The fate of the adjacent motion segments after lumbar fusion. *J Spinal Disord Tech* 2003;16:338–45. [PubMed: 12902949]
2. Ghiselli G, Wang JC, Bhatia NN, et al. Adjacent segment degeneration in the lumbar spine. *J Bone Joint Surg Am* 2004;86-A:1497–503. [PubMed: 15252099]



3. Cheh G, Bridwell KH, Lenke LG, et al. Adjacent segment disease following lumbar/thoracolumbar fusion with pedicle screw instrumentation: a minimum 5-year follow-up. *Spine* 2007;32:2253–7. [PubMed: 17873819]
4. Allen MJ, Schoonmaker JE, Bauer TW, et al. Preclinical evaluation of a poly (vinyl alcohol) hydrogel implant as a replacement for the nucleus pulposus. *Spine* 2004;29:515–23. [PubMed: 15129064]
5. Bao QB, Yuan HA. New technologies in spine: nucleus replacement. *Spine* 2002;27:1245–7. [PubMed: 12045526]
6. Eysel P, Rompe J, Schoenmayr R, et al. Biomechanical behaviour of a prosthetic lumbar nucleus. *Acta Neurochir (Wien)* 1999;141:1083–7. [PubMed: 10550653]
7. Husson JL, Korge A, Polard JL, et al. A memory coiling spiral as nucleus pulposus prosthesis: concept, specifications, bench testing, and first clinical results. *J Spinal Disord Tech* 2003;16:405–11. [PubMed: 12902957]
8. Di Martino A, Vaccaro AR, Lee JY, et al. Nucleus pulposus replacement: basic science and indications for clinical use. *Spine* 2005;30:S16–S22. [PubMed: 16103829]
9. Bertagnoli R, Kumar S. Indications for full prosthetic disc arthroplasty: a correlation of clinical outcome against a variety of indications. *Eur Spine J* 2002;11 (Suppl 2):S131–S136. [PubMed: 12384734]
10. Cinotti G, David T, Postacchini F. Results of disc prosthesis after a minimum follow-up period of 2 years. *Spine* 1996;21:995–1000. [PubMed: 8726204]
11. Buttermann GR, Beaubien BP. Spinal load sharing of a compressible annulus sparing disc prosthesis. *The Spine Journal* 2004;4:S4–S5.
12. Buttermann GR, Beaubien BP. Stiffness of prosthetic nucleus determines stiffness of reconstructed lumbar calf disc. *Spine J* 2004;4:265–74. [PubMed: 15125847]
13. Ghiselli G, Wang JC, Hsu WK, et al. L5-S1 segment survivorship and clinical outcome analysis after L4–L5 isolated fusion. *Spine* 2003;28:1275–80. [PubMed: 12811271]
14. Kramer PA. Prevalence and distribution of spinal osteoarthritis in women. *Spine* 2006;31:2843–8. [PubMed: 17108839]
15. Kettler A, Wilke HJ. Review of existing grading systems for cervical or lumbar disc and facet joint degeneration. *Eur Spine J* 2006;15:705–18. [PubMed: 16172902]
16. Wilke HJ, Rohlmann F, Neidlinger-Wilke C, et al. Validity and interobserver agreement of a new radiographic grading system for intervertebral disc degeneration: Part I. Lumbar spine. *Eur Spine J* 2006;15:720–30. [PubMed: 16328226]
17. Beaubien BP, Derincek A, Lew WD, et al. In vitro, biomechanical comparison of an anterior lumbar interbody fusion with an anteriorly placed, low-profile lumbar plate and posteriorly placed pedicle screws or translamina screws. *Spine* 2005;30:1846–51. [PubMed: 16103854]
18. Crompton PA, Bruhlmann SB, Orr TE, et al. In vitro axial preload application during spine flexibility testing: towards reduced apparatus-related artefacts. *J Biomech* 2000;33:1559–68. [PubMed: 11006379]
19. Buttermann, GR. Annulus Sparing Lumbar Disc Prosthesis Stability and Motion Preservation in an In Vivo Animal Model. 6th Annual Meeting of the Spine Arthroplasty Society; Montreal, Canada. 2006.
20. Proctor CS, Schmidt MB, Whipple RR, et al. Material properties of the normal medial bovine meniscus. *J Orthop Res* 1989;7:771–82. [PubMed: 2677284]
21. Thompson JP, Pearce RH, Schechter MT, et al. Preliminary evaluation of a scheme for grading the gross morphology of the human intervertebral disc. *Spine* 1990;15:411–5. [PubMed: 2363069]
22. Nachemson AL, Elfstrom G. Intravital dynamic pressure measurements in lumbar discs. A study of common movements, maneuvers and exercises. *Scand J Rehabil Med Suppl* 1970;1:1–40. [PubMed: 4257209]
23. Schultz A, Andersson G, Ortengren R, et al. Loads on the lumbar spine. Validation of a biomechanical analysis by measurements of intradiscal pressures and myoelectric signals. *J Bone Joint Surg Am* 1982;64:713–20. [PubMed: 7085696]
24. Nachemson A. Lumbar intradiscal pressure. Experimental studies on post-mortem material. *Acta Orthop Scand Suppl* 1960;43:1–104. [PubMed: 14425680]

25. Koeller W, Muehlhaus S, Meier W, et al. Biomechanical properties of human intervertebral discs subjected to axial dynamic compression--influence of age and degeneration. *J Biomech* 1986;19:807–16. [PubMed: 3782163]
26. Shao Z, Rompe G, Schiltenswolf M. Radiographic changes in the lumbar intervertebral discs and lumbar vertebrae with age. *Spine* 2002;27:263–8. [PubMed: 11805689]
27. Tibrewal SB, Pearcy MJ. Lumbar intervertebral disc heights in normal subjects and patients with disc herniation. *Spine* 1985;10:452–4. [PubMed: 4049112]
28. Walsh AJ, Lotz JC. Biological response of the intervertebral disc to dynamic loading. *J Biomech* 2004;37:329–37. [PubMed: 14757452]
29. Court C, Chin JR, Liebenberg E, et al. Biological and mechanical consequences of transient intervertebral disc bending. *Eur Spine J.* 2007
30. Kroeber M, Unglaub F, Guegring T, et al. Effects of controlled dynamic disc distraction on degenerated intervertebral discs: an in vivo study on the rabbit lumbar spine model. *Spine* 2005;30:181–7. [PubMed: 15644753]
31. Guehring T, Omlor GW, Lorenz H, et al. Disc distraction shows evidence of regenerative potential in degenerated intervertebral discs as evaluated by protein expression, magnetic resonance imaging, and messenger ribonucleic acid expression analysis. *Spine* 2006;31:1658–65. [PubMed: 16816759]
32. Hirsch C. The reaction of intervertebral discs to compression forces. *J Bone Joint Surg Am* 1955;37-A:1188–96. [PubMed: 13271464]
33. Koeller W, Meier W, Hartmann F. Biomechanical properties of human intervertebral discs subjected to axial dynamic compression. A comparison of lumbar and thoracic discs. *Spine* 1984;9:725–33. [PubMed: 6505843]
34. Lin HS, Liu YK, Adams KH. Mechanical response of the lumbar intervertebral joint under physiological (complex) loading. *J Bone Joint Surg Am* 1978;60:41–55. [PubMed: 624758]
35. Markolf KL, Morris JM. The structural components of the intervertebral disc. A study of their contributions to the ability of the disc to withstand compressive forces. *J Bone Joint Surg Am* 1974;56:675–87. [PubMed: 4835815]
36. Smeathers JE, Joanes DN. Dynamic compressive properties of human lumbar intervertebral joints: a comparison between fresh and thawed specimens. *J Biomech* 1988;21:425–33. [PubMed: 3417694]
37. Brown T, Hansen RJ, Yorra AJ. Some mechanical tests on the lumbosacral spine with particular reference to the intervertebral discs; a preliminary report. *J Bone Joint Surg Am* 1957;39-A:1135–64. [PubMed: 13475413]
38. Hirsch C, Nachemson A. New observations on the mechanical behavior of lumbar discs. *Acta Orthop Scand* 1954;23:254–83. [PubMed: 13206726]
39. Langrana NA, Parsons JR, Lee CK, et al. Materials and design concepts for an intervertebral disc spacer. I. fiber-reinforced composite design. *J Appl Biomater* 1994;5:125–32. [PubMed: 10172071]
40. Markolf KL. Deformation of the thoracolumbar intervertebral joints in response to external loads: a biomechanical study using autopsy material. *J Bone Joint Surg Am* 1972;54:511–33. [PubMed: 5055150]
41. Shea M, Takeuchi TY, Wittenberg RH, et al. A comparison of the effects of automated percutaneous discectomy and conventional discectomy on intradiscal pressure, disk geometry, and stiffness. *J Spinal Disord* 1994;7:317–25. [PubMed: 7949699]
42. Joshi A, Mehta S, Vresilovic E, et al. Nucleus implant parameters significantly change the compressive stiffness of the human lumbar intervertebral disc. *J Biomech Eng* 2005;127:536–40. [PubMed: 16060361]
43. Andersson GB, Schultz AB. Effects of fluid injection on mechanical properties of intervertebral discs. *J Biomech* 1979;12:453–8. [PubMed: 457699]
44. Lindsey DP, Swanson KE, Fuchs P, et al. The effects of an interspinous implant on the kinematics of the instrumented and adjacent levels in the lumbar spine. *Spine* 2003;28:2192–7. [PubMed: 14520030]
45. Nachemson AL, Schultz AB, Berkson MH. Mechanical properties of human lumbar spine motion segments. Influence of age, sex, disc level, and degeneration. *Spine* 1979;4:1–8. [PubMed: 432710]

46. Panjabi MM, Oxland TR, Yamamoto I, et al. Mechanical behavior of the human lumbar and lumbosacral spine as shown by three-dimensional load-displacement curves. *J Bone Joint Surg Am* 1994;76:413–24. [PubMed: 8126047]
47. Pearcy MJ, Tibrewal SB. Axial rotation and lateral bending in the normal lumbar spine measured by three-dimensional radiography. *Spine* 1984;9:582–7. [PubMed: 6495028]
48. Schendel MJ, Wood KB, Buttermann GR, et al. Experimental measurement of ligament force, facet force, and segment motion in the human lumbar spine. *J Biomech* 1993;26:427–38. [PubMed: 8478347]
49. Schultz AB, Warwick DN, Berkson MH, et al. Mechanical properties of human lumbar spine motion segments: I. Responses in flexion, extension, lateral bending, and torsion. *J Biomech Eng* 1979;101:46–52.
50. Eijkelkamp MF, van Donkelaar CC, Veldhuizen AG, et al. Requirements for an artificial intervertebral disc. *Int J Artif Organs* 2001;24:311–21. [PubMed: 11420881]
51. Steffen T, Rubin RK, Baramki HG, et al. A new technique for measuring lumbar segmental motion in vivo. Method, accuracy, and preliminary results. *Spine* 1997;22:156–66. [PubMed: 9122795]
52. Bible JE, Simpson AK, Emerson JW, et al. Quantifying the effects of degeneration and other patient factors on lumbar segmental range of motion using multivariate analysis. *Spine* 2008;33:1793–9. [PubMed: 18628713]
53. Quint U, Wilke HJ. Grading of degenerative disk disease and functional impairment: imaging versus patho-anatomical findings. *Eur Spine J* 2008 Dec;17(12):1705–13. [PubMed: 18839226]
54. Mimura M, Panjabi MM, Oxland TR, et al. Disc degeneration affects the multidirectional flexibility of the lumbar spine. *Spine* 1994;19:1371–80. [PubMed: 8066518]
55. Zhao F, Pollintine P, Hole BD, et al. Discogenic origins of spinal instability. *Spine* 2005;30:2621–30. [PubMed: 16319748]
56. Panjabi MM. The stabilizing system of the spine. Part II. Neutral zone and instability hypothesis. *J Spinal Disord* 1992 Dec;5(4):390–6. [PubMed: 1490035]
57. Havey, R.; Voronov, L.; Gaitanis, I., et al. Relaxation response of lumbar spine segments undergoing annular distraction: Implications to anterior lumbar interbody implant stability. 50th annual meeting of the Orthopaedic Research Society; San Francisco, CA. Mar. 2004
58. Wilke HJ, Jungkunz B, Wenger K, et al. Spinal segment range of motion as a function of in vitro test conditions: effects of exposure period, accumulated cycles, angular-deformation rate, and moisture condition. *Anat Rec* 1998;251:15–9. [PubMed: 9605215]
59. Lipman, J.; Campbell, D.; Girardi, F., et al. Mechanical behavior of the ProDisc II intervertebral disc prosthesis in human cadaveric spines. 49th Annual Meeting of the Orthopaedic Research Society; New Orleans, LA. Feb 2–5; 2003.
60. O’Leary P, Nicolakis M, Lorenz MA, et al. Response of Charite total disc replacement under physiologic loads: prosthesis component motion patterns. *Spine J* 2005;5:590–9. [PubMed: 16291097]
61. Cunningham BW, Dmitriev AE, Hu N, et al. General principles of total disc replacement arthroplasty: seventeen cases in a nonhuman primate model. *Spine* 2003;28:S118–S124. [PubMed: 14560183]
62. Panjabi M, Henderson G, Abjornson C, et al. Multidirectional testing of one- and two-level ProDisc-L versus simulated fusions. *Spine* 2007;32:1311–9. [PubMed: 17515820]
63. Huang RC, Girardi FP, Cammisa FP Jr, et al. The implications of constraint in lumbar total disc replacement. *J Spinal Disord Tech* 2003;16:412–7. [PubMed: 12902958]
64. McAfee PC, Cunningham BW, Hayes V, et al. Biomechanical analysis of rotational motions after disc arthroplasty: implications for patients with adult deformities. *Spine* 2006;31:S152–S160. [PubMed: 16946633]

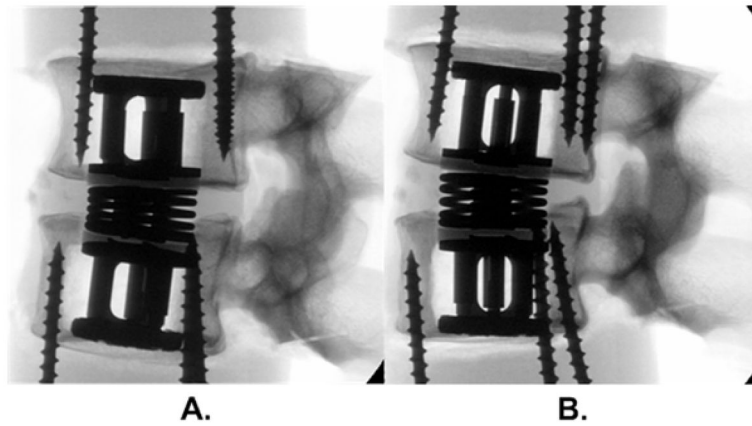


**Figure 1.**

Radiographs of an annulus-sparing prosthesis (Dynamic Spine Inc., CA USA) in (a) flexion and (b) extension load states. This prosthesis has an expandable component inserted in the adjacent vertebral bodies which gives a preload of the compressible spring component in the nuclear space. This when combined with the intact annulus aims to restore compressive and bending properties of the disc. Fibrous tissue ingrowth is expected within the coil springs, and was represented in this study using household silicone sealant. The long screws are not part of the device, they were used to hold the vertebrae to the epoxy potting material.

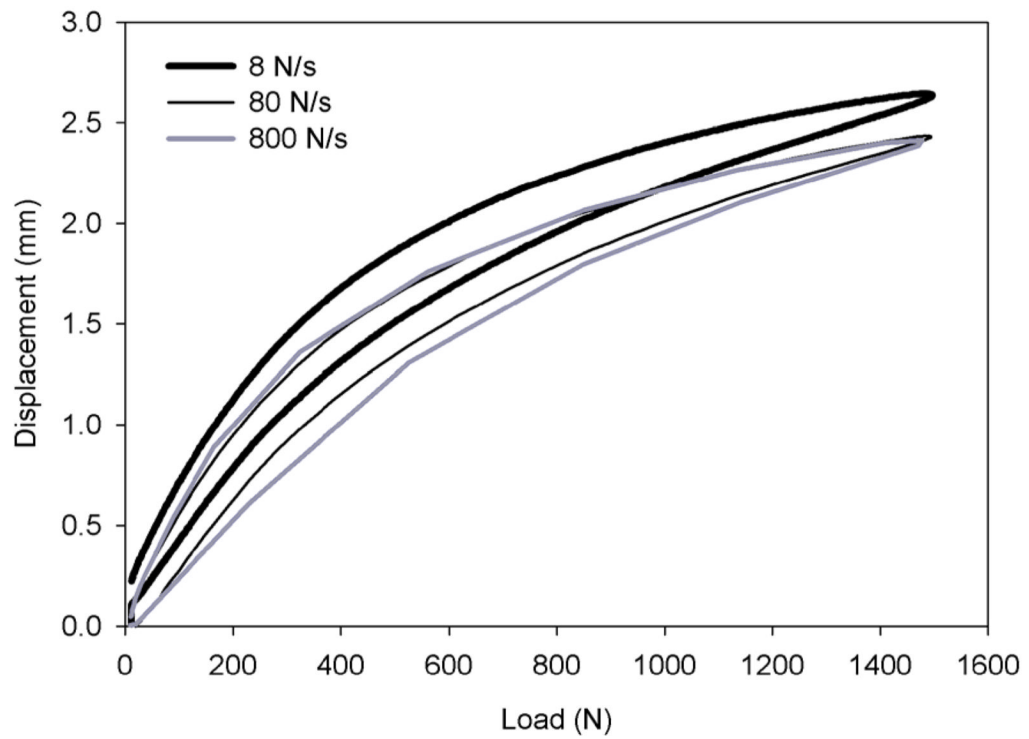


**Figure 2.** Mean axial compression load-displacement characteristics of IPD reconstructed discs at load rates of 8, 80, and 800 N/sec. Differences between the curves was minimal at loading rates greater than 80 N/s.



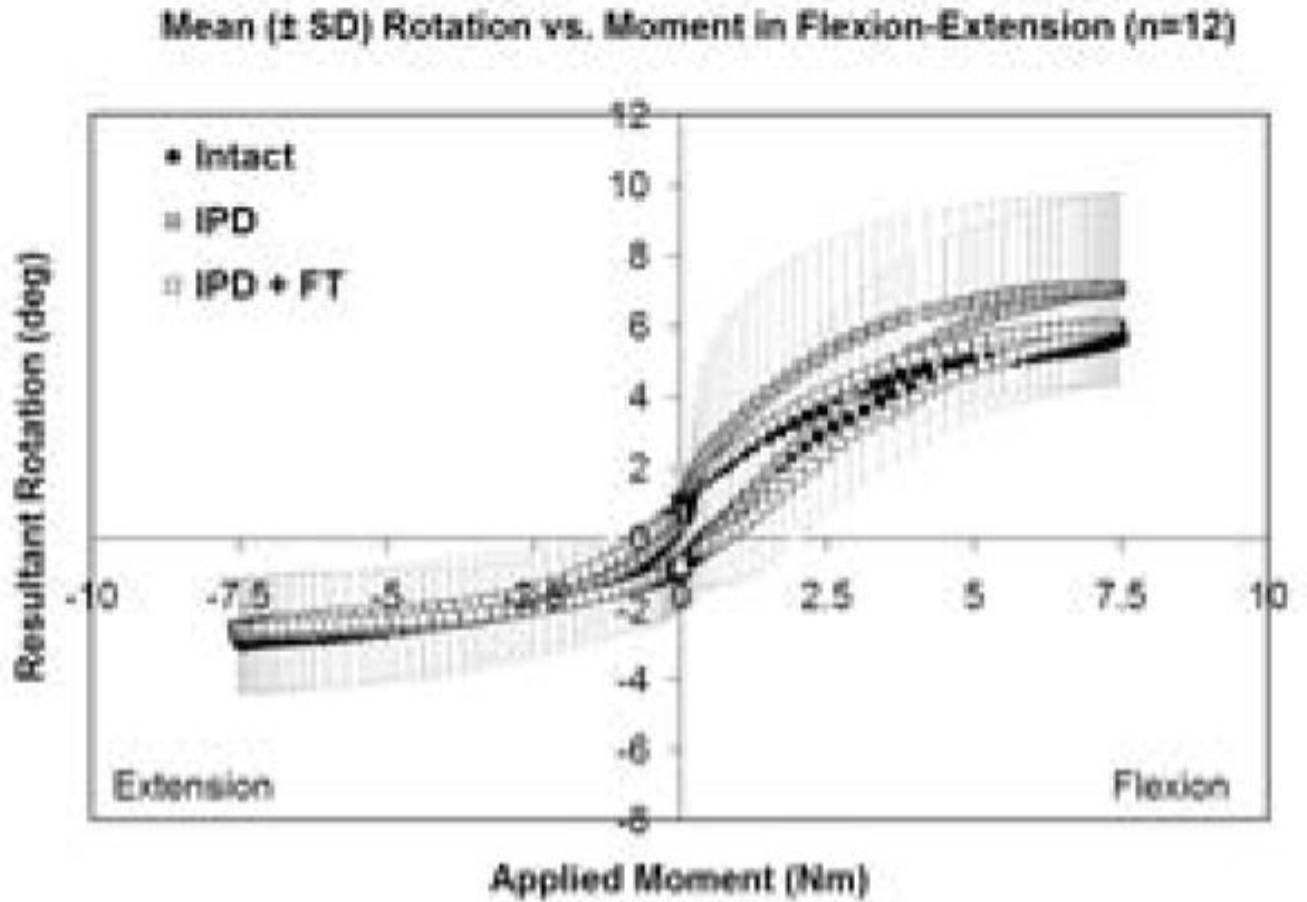


**Figure 3.** Mean flexion-extension flexibility curves for intact, IPD reconstructed, and IPD reconstructed discs with simulated fibrous tissue (FT). Error bars representing one standard deviation are shown only for the IPD state. The amount of variation was similar for all groups.

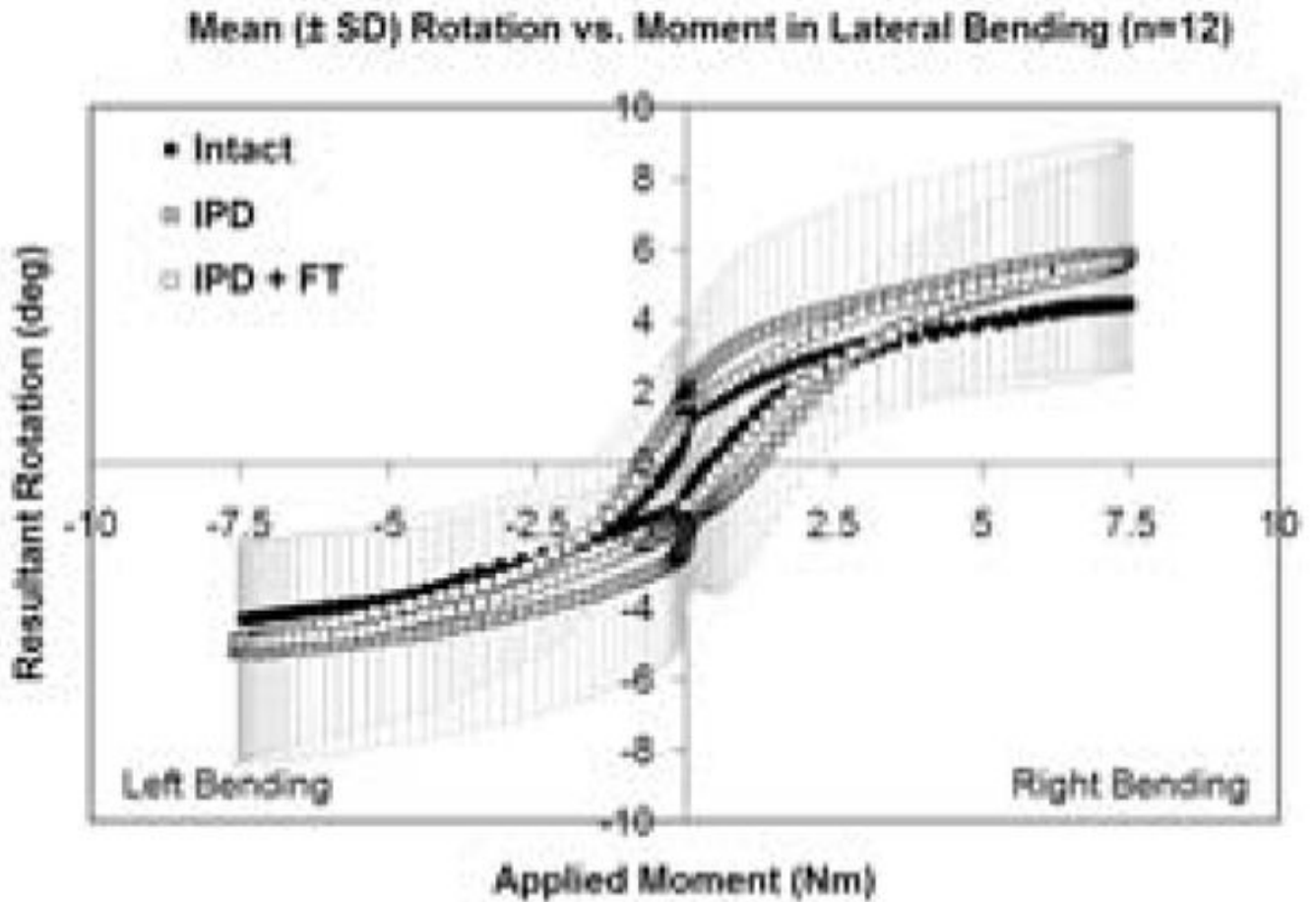


**Figure 4.**

Mean combined right and left lateral bending flexibility curves for intact, IPD reconstructed, and IPD reconstructed discs with simulated fibrous tissue (FT). Error bars representing one standard deviation are shown only for the IPD state. The amount of variation was similar for all groups.

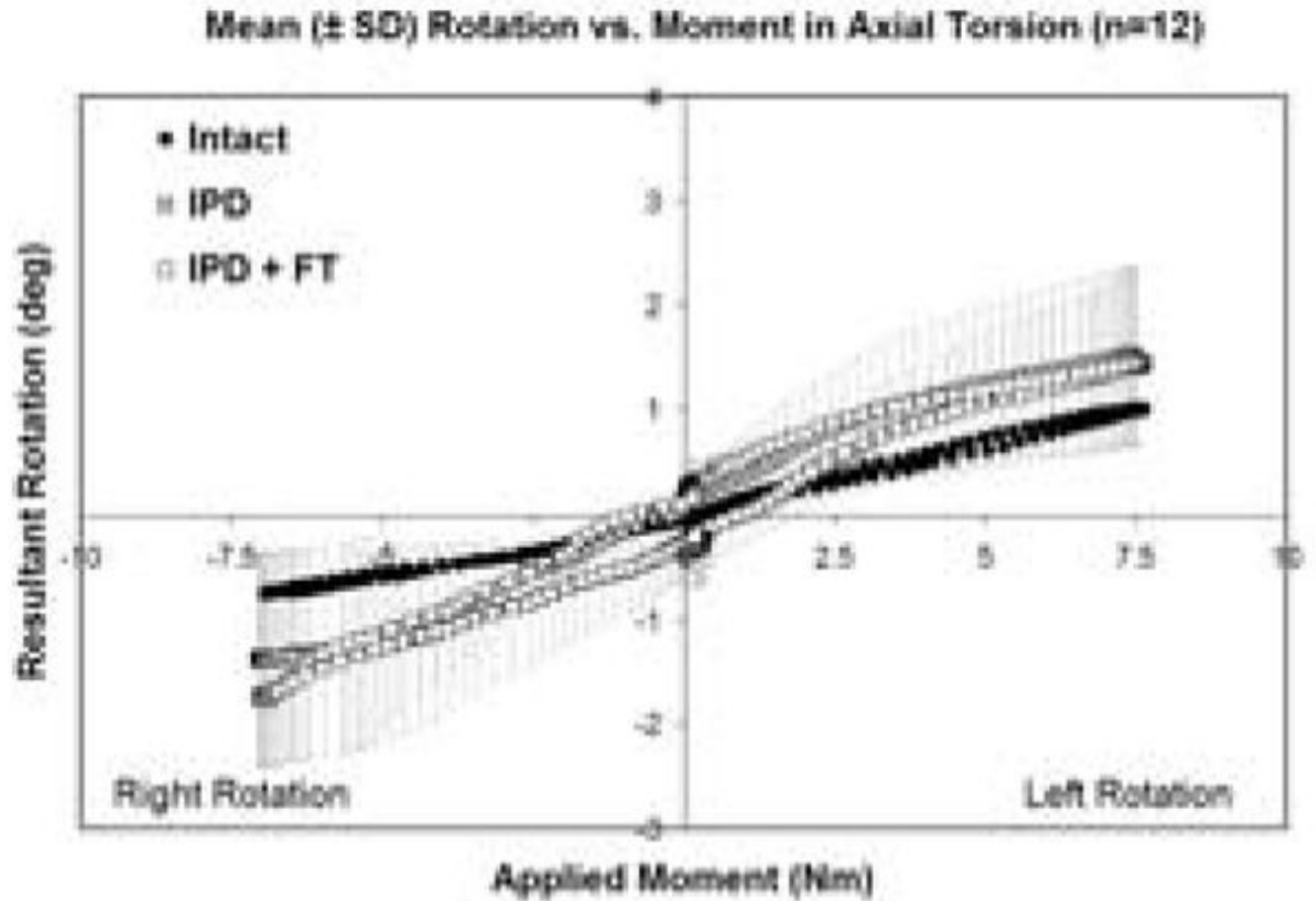


**Figure 5.** Mean axial torsion load-displacement flexibility curves for intact, IPD reconstructed, and IPD reconstructed discs with simulated fibrous tissue (FT). Error bars representing one standard deviation are shown only for the IPD state. The amount of variation was similar for all groups.

## Flexion-Extension Range of Motion and Neutral Zone

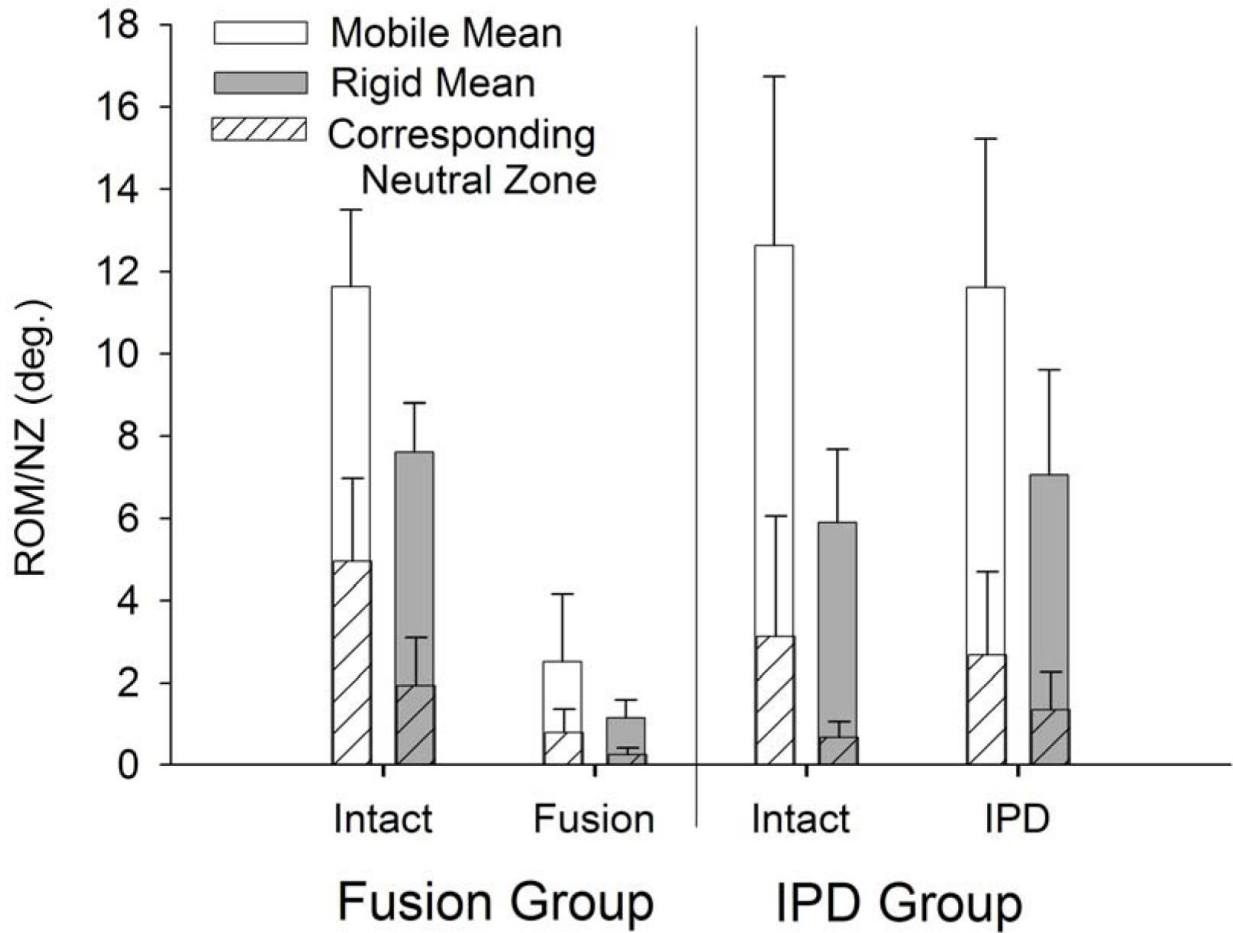


**Figure 6.** Flexion-Extension range-of-motion and neutral zone (mean  $\pm$  standard deviation) for intact and reconstructed discs in the IPD (with simulated fibrous tissue) and fusion groups stratified to mobile (intact flexion-extension ROM  $> 9^\circ$ ) and rigid (intact flexion-extension ROM  $< 9^\circ$ ) groups.

## Lateral Bending Range of Motion and Neutral Zone

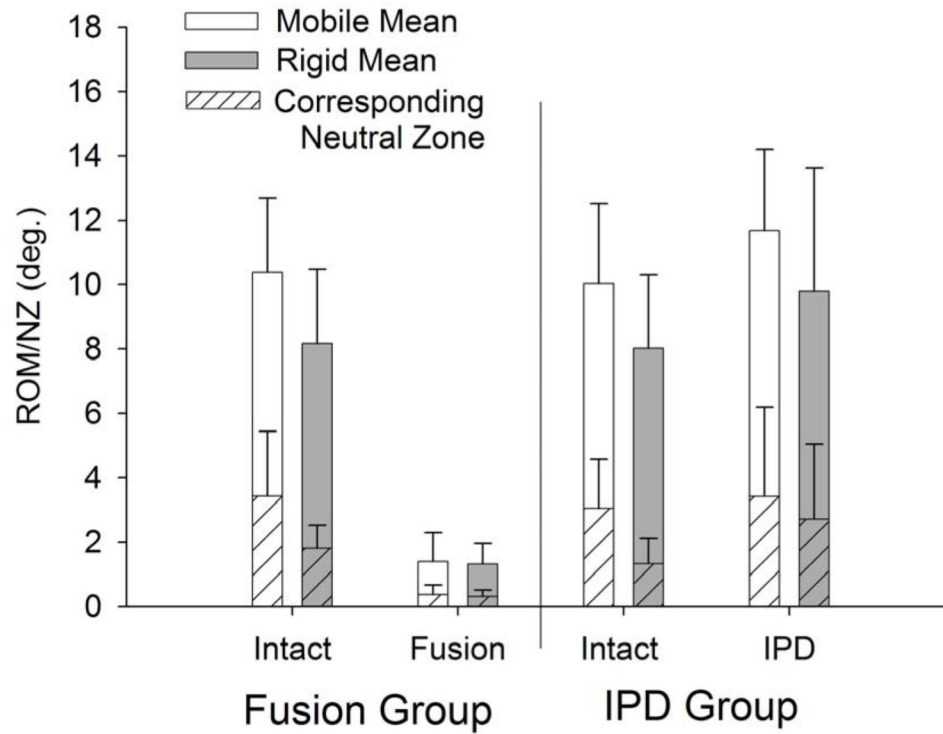


**Figure 7.** Bilateral lateral bending range-of-motion and neutral zone (mean  $\pm$  standard deviation) for intact and reconstructed discs in the IPD (with simulated fibrous tissue) and fusion groups stratified to mobile (intact flexion-extension ROM  $> 9^\circ$ ) and rigid (intact flexion-extension ROM  $< 9^\circ$ ) groups.



## Axial Torsion Range of Motion and Neutral Zone

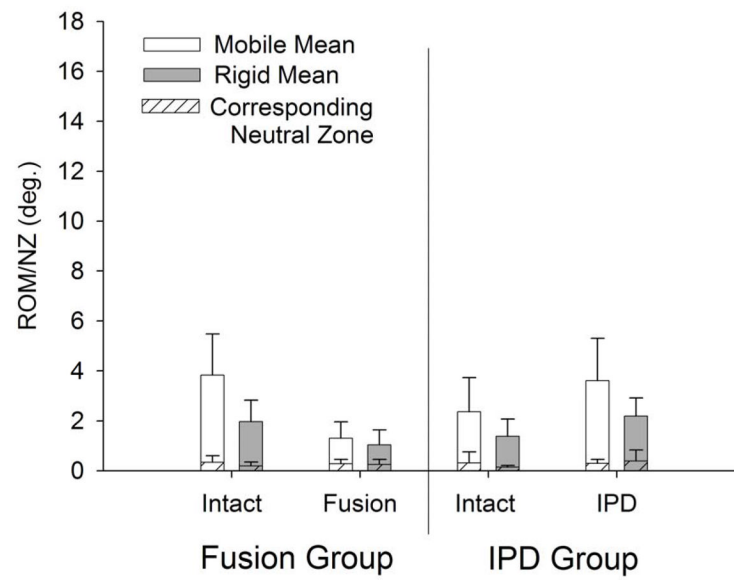


**Figure 8.** Bilateral axial torsion range-of-motion and neutral zone (mean  $\pm$  standard deviation) for intact and reconstructed discs in the IPD (with simulated fibrous tissue) and fusion groups stratified to mobile (intact flexion-extension ROM  $> 9^\circ$ ) and rigid (intact flexion-extension ROM  $< 9^\circ$ ) groups.

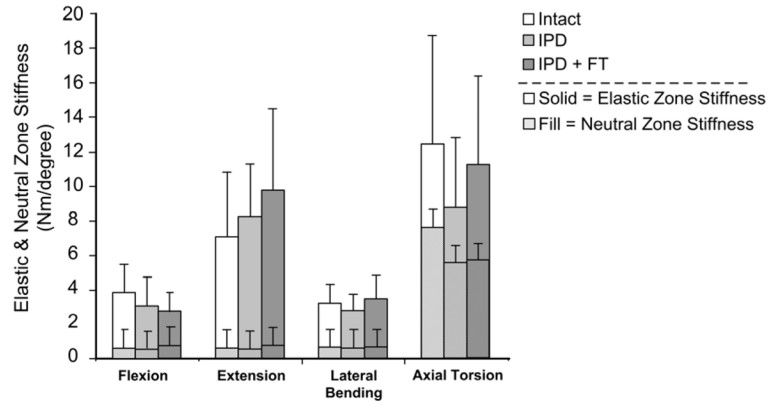


**Figure 9.**

Initial and elastic zone stiffness (mean  $\pm$  standard deviation) for intact, IPD reconstructed, and IPD reconstructed disc with simulated fibrous tissue (FT). Neutral zone stiffness was the same for flexion vs. extension and is plotted in front of the elastic zone stiffness for both test directions. IPD reconstructed tended to slightly increase extension elastic zone stiffness and to decrease torsion neutral zone stiffness. These trends were not statistically significant.

**Table**  
 Characteristics of the intact specimens prior to instrumentation. Numerical values represent mean  $\pm$  SD.

	Fusion		Intervertebral Prosthetic Disc (IPD)		P Values	
	Mobile	Rigid	Mobile	Rigid	Rigid vs. Mobile	Fusion vs. IPD
<b>Demographic information</b>						
Age	49.3 $\pm$ 9.3	52.4 $\pm$ 6.7	42.6 $\pm$ 3.2	49.3 $\pm$ 5.0	0.037	0.065
Sex	71% Male	70% Male	100% Male	100% Male		N/A
Weight (kg)	65 $\pm$ 20*	53 $\pm$ 14	96 $\pm$ 37	83 $\pm$ 15	0.26	0.003
Height (cm)	172 $\pm$ 9	169 $\pm$ 7	178 $\pm$ 9	190 $\pm$ 15	0.365	0.006
<b>Anterior disc height</b>	11.0 $\pm$ 2.3	8.4 $\pm$ 1.5	13.0 $\pm$ 2.7	11.9 $\pm$ 1.5	0.013	0.001
<b>Disc height/diameter ratio</b>	0.37 $\pm$ 0.08	0.27 $\pm$ 0.03	0.35 $\pm$ 0.08	0.29 $\pm$ 0.02	0.003	0.981
<b>DEXA score</b>	1.07 $\pm$ 0.13	1.07 $\pm$ 0.20	1.08 $\pm$ 0.10	1.27 $\pm$ 0.24	0.018	0.123
<b>Disc degeneration</b>						
Radiographic	2.2 $\pm$ 0.8	1.9 $\pm$ 0.5	2.2 $\pm$ 0.3	2.6 $\pm$ 0.9		Global p>0.25
Gross Morphology			1.2 $\pm$ 0.4	2.3 $\pm$ 1.0	0.046	NA
<b>Facet degeneration</b>						
Radiographic	2.4 $\pm$ 0.5	1.9 $\pm$ 0.6	2.4 $\pm$ 0.4	2.5 $\pm$ 0.5		Global p>0.14